

Structure, surface acidity and catalytic activity of WO₃-TiO₂ catalyst for NH₃-SCR of NO_x

Byeongkil Shin^a, Teng Wan Dung^b and Heesoo Lee^{a,*}

^aSchool of Materials Science and Engineering, Pusan National University, Busan 609-735, Korea

^bCeramics Technology Group, SIRIM Berhad, 1 Persiaran Dato Menteri, 40911 Shah Alam, Selangor, Malaysia

WO₃-TiO₂ catalysts were prepared by an incipient wet-impregnation method for high-temperature selective catalytic reduction (SCR) of NO_x. Structure, surface acidity, and catalytic performance of SCR catalyst according to WO₃ content (4, 6, 8, and 10 wt.%) were characterized by morphological and spectroscopy analyses. The 10 wt.% WO₃-TiO₂ catalyst had high conversion efficiency due to the improvement of specific surface area, catalytic acidity, and monolayer capacity of TiO₂ support. It was found that tungsten oxide species are dispersed in the interlayer between the grain and the grain boundary of TiO₂ support in transmission electron microscopy. The WO₃ affected the suppressed grain growth and the improved Brønsted acid sites that could provide much surface acidity by the grain boundary reinforcement. The structural interaction between the proper WO₃ content and TiO₂ support led to the existence of octahedrally and tetrahedrally coordinated WO₃ structures on the surface in the Raman spectra. The enhanced catalytic activity of 10 wt.% WO₃-TiO₂ is attributed to the increase of the surface acidity (Brønsted acid sites) by the shell formation of WO₃ species.

Key words: WO₃-TiO₂ SCR catalysts, Surface acidity, Catalytic activity, Shell formation, Grain boundary reinforcement.

Introduction

The selective catalytic reduction (SCR) of NO_x by NH₃ is an efficient technology to reduce NO_x emission in flue gas from stationary sources, which is one of the most convenient, effective, and economical method. The SCR catalysts are generally designed to operate in the temperature range between 300 and 450 °C [1, 2]. Since the catalytic activity of the conventional catalyst decreases gradually on the long-term operation in exhaust gases, its durability is required for high temperature SCR over time [3].

The SCR catalyst with thermal stability is applicable for high temperature exhaust gases of 450-600 °C from mobile SCR system (i.e. diesel trucks, vessel, etc.) or some turbines [3-6]. The V₂O₅/TiO₂-based catalyst cannot be used at high temperatures because their catalytic activity significantly decreases above 500 °C, whereas the WO₃-TiO₂ or WO₃-V₂O₅-TiO₂ catalysts are known to exhibit high SCR activity and good thermal stability at these temperatures [5, 6].

The WO₃ as a promoter is used to enhance the NO conversion efficiency and the temperature window because it increased the amount and the strength of Brønsted acid sites on the catalyst surface [3, 7]. Several researchers have been primarily focused on a

chemical activity and phase transition of the catalyst systems for high temperature SCR [7-9]. It was reported that the high dispersion of the tungsten species achieved on the TiO₂ spheres, the strong interaction, and the medium-strong acidity are considered to contribute to the superior catalytic behavior of the SCR catalysts [10].

In this study, the effect of WO₃ content on catalytic activity for WO₃-TiO₂ catalysts was investigated to elucidate the thermal stability in the context of their catalytic acidity and monolayer capacity. The WO₃-TiO₂ catalysts with different WO₃ content were prepared by wet impregnation, and their crystal structure and surface acidity were characterized by morphological and spectroscopy analyses. The conversion efficiency of the SCR catalysts with different WO₃ content was observed in the temperature range 250-500 °C.

Experimental

Specimen preparation

The WO₃-TiO₂ SCR catalysts with 4-10 wt. % WO₃ content were prepared by the conventional incipient wetness impregnation method using a WO₃ precursor and the partially sulfated TiO₂ (96%, SO₃ -2%) as the support of catalysts. The TiO₂ powder with a specific surface area of 280 m²/g was synthesized from meta-titanic acid, and then the powder was heat-treated at 500 °C. Ammonium paratungstate-hydrate ((NH₄)₁₀(W₁₂O₄₁)·xH₂O) as a precursor of WO₃ was dissolved in hot distilled water. To prepare slurries, the solution

*Corresponding author:
Tel : +82-51-510-2388
Fax: +82-51-512-0528
E-mail: heesoo@pusan.ac.kr

and the TiO₂ powder were mixed and ball-milled for 12 h. The slurries were dried in oven at 130 °C for 24 h and the catalysts with different WO₃ content (4, 6, 8, and 10 wt.%) were obtained. The heat treatment for the thermal stability was carried out using a muffle furnace maintaining at 800 °C for 3 h.

Characterization

The NO_x conversion efficiency of the as-prepared catalysts in a presence of NH₃ was measured using a fixed bed reactor designed on basis of the guideline VGB-R 302 H e [11]. A feed consisting of 500 ppm NO, 600 ppm NH₃, and 6 vol.% O₂ (99.99%) with N₂ being the carrier gas were used. The conversion efficiency was observed in the temperature range 250–500 °C, and each temperature was maintained until steady-state conditions.

The crystal phase was analyzed using an X-ray diffractometer (M18XHF, MAC Science, Netherlands) as for the heat-treated catalysts. The effects of WO₃ addition on the morphology of the catalysts were examined by scanning electron microscope (SEM, S-4700, Hitachi, Japan) and transmission electron microscope (TEM, JEN 2100F, JEOL, Japan). The specific surface areas of catalysts were measured by BET (Brunauer-Emmett-Teller)-method (ASAP2010, Micromeritics, USA). The catalytic acidity and the monolayer capacity were determined by FT-IR (NH₃ atmosphere, wave number 2000–1000 cm⁻¹, Nicolet 6700, Thermo Scientific, USA) and Raman spectroscopy (Ar-Ion laser-514 nm, Raman System 2000, Renishaw, UK), respectively. TEM-EDS (energy dispersive spectrometry) analysis was used to identify the composition of core-shell region. EDS spectra were recorded in spot-profile analysis by focusing electron beam onto specific regions of particles.

Results and Discussion

The NO_x conversion efficiency for as-prepared catalysts is shown in Fig. 1. A change of the efficiency for the catalysts with the different WO₃ content was not remarkable under 400 °C, whereas the catalytic efficiency was abruptly reduced over 400 °C. In addition, the improvement of the efficiency with the WO₃ content could not be clearly confirmed, but degree of the

efficiency reduction decreased with the increase of WO₃ content at 500 °C. It is well known that the addition of WO₃ leads to the improvement of thermal stability and high performance for the SCR reaction and expansion of temperature window [12]. This result indicates that thermal stability of the WO₃-TiO₂ catalysts over the 400 °C is attributed to the addition of WO₃.

Table 1 shows the variation of specific surface areas and mean diameters of secondary particles for the catalysts as heated at 800 °C. It was reported that the addition of WO₃ inhibits a grain growth of TiO₂ and increases specific surface area in WO₃-TiO₂ catalysts [2, 4, 7]. As shown in Table 1, the size of secondary particle for the catalysts without the WO₃ content was

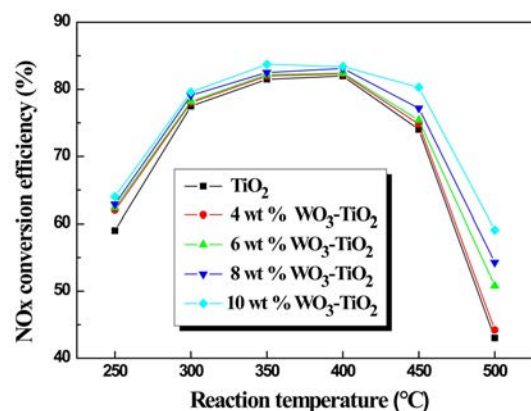


Fig. 1. NO_x conversion efficiency of the WO₃-TiO₂ catalysts with various tungsten oxides content. Reaction conditions: [NO] = 500 ppm, [NH₃] = 600 ppm, [O₂] = 6 vol. %, GHSV = 10,000 h⁻¹.

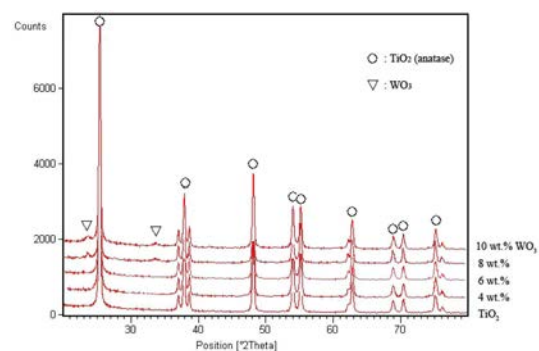


Fig. 2. XRD patterns of the WO₃-TiO₂ catalysts with different tungsten oxides content.

Table 1. Properties of the WO₃-TiO₂ catalysts with various WO₃ content.

Samples	WO ₃ loading (wt. %) (XRF)	Specific surface area (m ² /g)	Mean diameter of secondary particle (nm)
TiO ₂	None	31	660
4 wt. % WO ₃ -TiO ₂	4.3861	38	515
6 wt. % WO ₃ -TiO ₂	6.3028	39	484
8 wt. % WO ₃ -TiO ₂	8.4597	43	473
10 wt. % WO ₃ -TiO ₂	10.8027	44	471

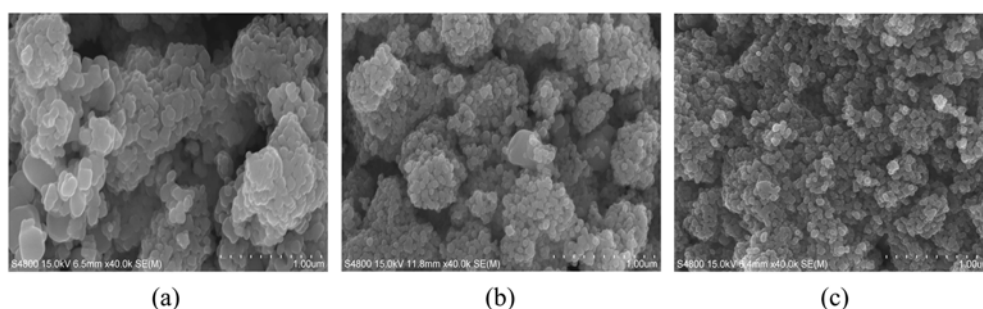


Fig. 3. SEM images of the powder with different WO_3 loadings. (a) without WO_3 , (b) 4 wt.% WO_3 , and (c) 10 wt.% WO_3 .

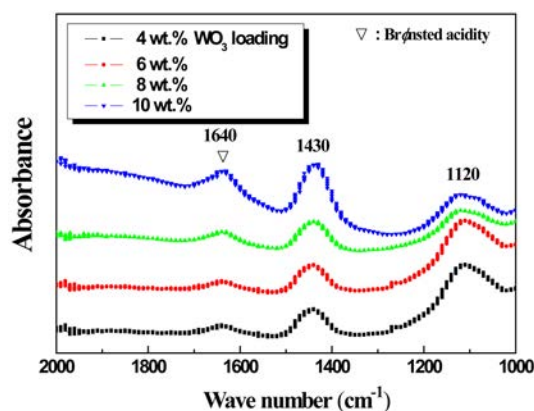


Fig. 4. FT-IR spectra of adsorbed ammonia in the range of 1000-2000 cm^{-1} recorded at room temperature for the WO_3 - TiO_2 catalysts with 4, 6, 8, and 10 wt.% WO_3 loadings.

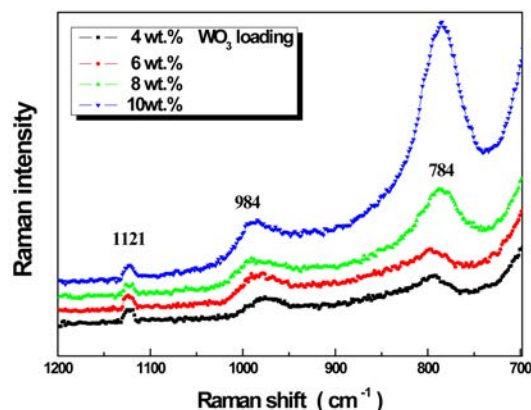


Fig. 5. Raman spectra of the WO_3 - TiO_2 catalysts with 4, 6, 8, and 10 wt.% WO_3 content.

660 nm and the reduction of the size of secondary particle was found from 515 nm to 471 nm as increased of the WO_3 content. The specific surface areas of the catalysts were increased by WO_3 addition.

The X-ray diffraction patterns of the WO_3 - TiO_2 catalysts with various WO_3 content are presented in Fig. 2. The peak of WO_3 was not detected for the catalyst with 4 wt.% WO_3 content. The anatase phase of TiO_2 was detected but the rutile phase was not observed. It indicated that tungsten species in WO_3 - TiO_2 catalysts were well-dispersed on TiO_2 with low crystallinity [12-14].

Fig. 3 shows the morphology of the WO_3 - TiO_2 catalysts as heated at 800 °C for 3 h. The particle size of the WO_3 - TiO_2 catalysts increased with the increase of calcination temperature. This result was consistent with the specific surface area as shown in table 1. The suppression of grain growth of the catalyst with 10 wt.% WO_3 - TiO_2 was observed at 800 °C, whereas that was not occurred without WO_3 content.

The adsorption activities of the WO_3 - TiO_2 catalysts with 4, 6, 8, and 10 wt.% WO_3 were measured by FT-IR of adsorbed NH_3 . In Fig. 4, the spectra show two distinct bands. The band around 1444 cm^{-1} indicates coordinated ammonia adsorbed on Lewis acid sites, and the other one is Brønsted acid sites which are corresponded to typical ammonium cations produced by ammonia protonation at 1640 cm^{-1} [3, 15-17]. In addition, the intensity of Brønsted and Lewis acid sites gradually increased with increasing WO_3 contents. Among them, Brønsted acid sites are associated with W-OH groups. It was reported that Brønsted acid sites were present in catalysts with WO_3 and not detected in a pure TiO_2 [16, 18]. Brønsted acid sites of the catalyst with 10 wt.% WO_3 content were higher than the catalyst with 4 wt.% WO_3 content. The increase of Brønsted acid sites improves the catalytic activity because tungstenyls centers act as adsorption sites for molecularly adsorbed ammonia. Consequently, the surface acidity and the catalytic activity were enhanced by the interaction of the tungsten oxide species with titania on the surface.

Fig. 5 presents Raman spectra of WO_3 - TiO_2 catalysts with 4-10 wt.% WO_3 content, which were heat-treated at 800 °C. The broad bands ranging from 950 to 1024 cm^{-1} , which are centered around 984 cm^{-1} and the broad band around 790 cm^{-1} are ascribed to the existence of polymeric tungsten oxide species which are tetrahedrally and octahedrally coordinated [19-21]. The strong peak at 784 cm^{-1} consists of second-order anatase and WO_3 crystalline, in which tungsten atoms have octahedral coordination at high W concentration. The more the WO_3 content in WO_3 - TiO_2 catalysts, the higher the intensity of the peak around 784 cm^{-1} became. The peak due to crystalline WO_3 was faintly observed for WO_3 - TiO_2 catalysts with 4 and 6 wt.% WO_3 , whereas the peak became more obvious for

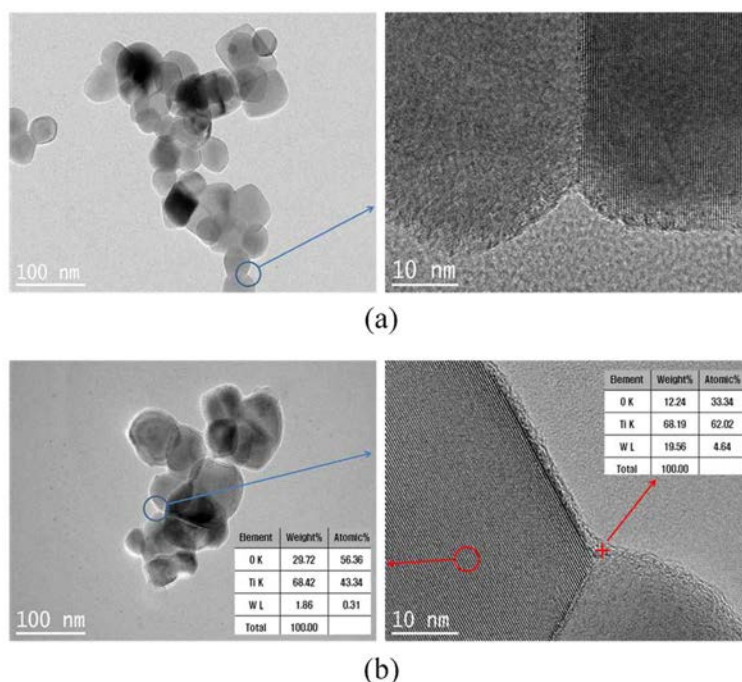


Fig. 6. TEM micrograph and EDS spot profiles of the WO_3 - TiO_2 catalysts with different WO_3 content: (a) 4 wt.% and (b) 10 wt.%.

WO_3 - TiO_2 catalysts with 10 wt.% WO_3 . The observed peak intensity with increasing WO_3 content was attributed to the change of coordination in W species to octahedral.

Fig. 6 shows TEM micrographs and EDS spot profiles of the heat-treated catalysts at 800 °C with 4 and 10 wt.% WO_3 loadings. A shell region distinguished from a core area was also observed at the grain boundary. The EDS spot profile was carried out in order to identify the tungsten oxide species on the grain boundary, and it indicated that the concentration of the WO_3 species was higher in the shell region than the core area. This suggests that the amorphous layer of tungsten oxide species have covered on the TiO_2 surface after heat treatment. It has been reported that increasing of the amount of WO_3 loading in TiO_2 particle suppressed the subsequent growth of the particles, and this suppression tend to increase in specific surface area [3, 8, 22]. In the present study, the enhanced catalytic properties of WO_3 - TiO_2 catalyst were attributed by the shell formation containing WO_3 , which led to the suppression of grain growth and the improvement of surface acidity [7, 23].

Conclusions

The effects of additive WO_3 on catalytic activity over the WO_3 - TiO_2 catalysts were examined by FT-IR, Raman, and TEM-EDS analyses. The results presented that WO_3 - TiO_2 catalyst is considerably dependent on temperature range and WO_3 content in SCR reaction. The catalyst with 10 wt.% WO_3 content showed

higher NO_x conversion efficiency than the others. The enhancement of specific surface area, surface acidity (Brønsted acid sites), and monolayer capacity of the WO_3 - TiO_2 catalysts were observed as the increase of WO_3 content. TEM-EDS analysis indicated that the core area was clearly distinguished from the shell region in terms of the existence of WO_3 boundaries, and this shell formation led to the suppression of grain growth and the improvement of catalytic activity. Thus, the addition of WO_3 reinforced the surface acidity due to the octahedrally and tetrahedrally coordinated WO_3 structures at the grain boundary.

Acknowledgments

This work was supported by the National Research Foundation of Korea (NRF) grant funded by the Korea government (MSIP) through GCRC-SOP (No. 2011-0030013).

References

1. P. Forzatti, *Appl. Catal. A-Gen.* 222 (2001) 221-236.
2. L. Lietti, J. Svachula, P. Forzatti, G. Ramis, P. Bregani, *Catal. Today.* 17 (1993) 131-139.
3. M. Kobayashi, K. Miyoshi, *Appl. Catal. B-Environ.* 72 (2007) 253-261.
4. J. Engweiler, J. Harf, A. Baiker, *J. Catal.* 159 (1996) 259-269.
5. M.C. Paganini, L. Dall'Acqua, E. Giamello, L. Lietti, P. Forzatti, *J. Catal.* 166 (1997) 195-205.
6. F. Nakajima, I. Hamada, *Catal. Today.* 29 (1996) 109-115.
7. E. Tronconi, I. Nova, C. Ciardelli, D. Chatterjee, M.

- Weibel, J. *Catal.* 245 (2007) 1-10.
8. G. Madia, M. Elsener, M. Koebel, F. Raimondi, A. Wokaun, *Appl. Catal. B-Environ.* 39 (2002) 181-190.
 9. S.T. Choo, S.D. Yim, I.-S. Nam, S.-W. Ham, J.-B. Lee, *Appl. Catal. B-Environ.* 44 (2003) 237-252.
 10. X. Yang, W. Dai, C. Guo, H. Chen, Y. Cao, H. Li, H. He, K. Fan, *J. Catal.* 234 (2005) 438-450.
 11. VGB guideline VGB-R 302 H e: guideline for the testing of DeNOx catalysts. Second ed., VGB, Essen (1998).
 12. S.M. Jung, P. Grange, *Appl. Catal. B-Environ.* 32 (2001) 123-131.
 13. G. Ramis, F. Bregani, *Catal. Lett.* 18 (1993) 299-303.
 14. S. Djerad, L. Tifouti, M. Crocoll, W. Weisweiler, 208 (2004) 257-265.
 15. G. Ramis, C. Cristiani, A.S. Elmi, P. Villa, *J. Mol. Catal.* 61 (1990) 319-331.
 16. M. Kobayashi, M. Hagi, *Appl. Catal. B-Environ.* 63 (2006) 104-113.
 17. B.H. Davis, R.A. Keogh, S. Alerasool, D.J. Zalewski, D.E. Day, P.K. Doolin, *J. Catal.* 183 (1999) 45-52.
 18. P. Patrono, A. La Ginestra, G. Ramis, *Appl. Catal. A-Gen.* 107 (1994) 249-266.
 19. V. Kumar, N. Lee, C.B. Almquist, *Appl. Catal. B-Environ.* 69 (2006) 101-114.
 20. K.K. Akurati, A. Vital, J.-P. Dellemann, K. Michalow, T. Graule, D. Ferri, A. Baiker, *Appl. Catal. B-Environ.* 79 (2008) 53-62.
 21. A. Scholz, B. Schnyder, A. Wokaun, *J. Mol. Catal. A-Chem.* 138 (1999) 249-261.
 22. G. Cristallo, E. Roncari, A. Rinaldo, F. Trifiro, *Appl. Catal. A-Gen.* 209 (2001) 249-256.
 23. W. Smith, Y.-P. Zhao, *Catal. Commun.* 10 (2009) 1117-1121.